6-2019

Dielectric Function Tensor (1.5 eV to 9.0 eV), Anisotropy, and Band to Band Transitions of Monoclinic β-(Al$_x$Ga$_{1-x}$)$_2$O$_3$ (x ≤ 0.21) Films

Matthew Hilfiker
University of Nebraska-Lincoln, mhilfiker2@huskers.unl.edu

Ufuk Kilic
University of Nebraska-Lincoln, ufukkilic@unl.edu

Alyssa Mock
Linköping University, alyssalynnmock@gmail.com

Vanya Darakchieva
Linköping University, Sweden, vanya.darakchieva@liu.se

Sean Knight
University of Nebraska-Lincoln, seanknight@unomaha.edu

Follow this and additional works at: https://digitalcommons.unl.edu/electricalengineeringfacpub

See next page for additional authors

Part of the Condensed Matter Physics Commons, and the Electrical and Computer Engineering Commons

Authors

Matthew Hilfiker, Ufuk Kilic, Alyssa Mock, Vanya Darakchieva, Sean Knight, Rafal Korlacki, Akhil Mauze, Yuewei Zhang, James Speck, and Mathias Schubert

Dielectric function tensor (1.5 eV to 9.0 eV), anisotropy, and band to band transitions of monoclinic #-(Al$_X$Ga$_{1-X}$)$_2$O$_3$ ($x \leq 0.21$) films

Matthew Hilfiker (iD), Ufuk Kilic (iD), Alyssa Mock (iD), Vanya Darakchieva (iD), Sean Knight (iD), $_{Rafał}$ Korlacki (iD), Akhil Mauze (iD), Yuewei Zhang (iD), James Speck, and Mathias Schubert (iD)

View Online   Export Citation   CrossMark

Dielectric function tensor (1.5 eV to 9.0 eV), anisotropy, and band to band transitions of monoclinic β-(Al$_x$Ga$_{1-x}$)$_2$O$_3$ ($x \leq 0.21$) films

Matthew Hilfiker,[1,a)] (iD) Ufuk Kilic,[1] (iD) Alyssa Mock,[2] (iD) Vanya Darakchieva,[2] (iD) Sean Knight,[1] (iD) Rafał Korlacki,[1] (iD)
Akhil Mauze,[3] (iD) Yuewei Zhang,[3] (iD) James Speck,[3] and Mathias Schubert[1,2,4] (iD)

AFFILIATIONS

[1]Department of Electrical and Computer Engineering, University of Nebraska-Lincoln, Lincoln, Nebraska 68588, USA
[2]Terahertz Materials Analysis Center and Center for III-N Technology, C3NiT – Janzèn, Department of Physics,
 Chemistry and Biology (IFM), Linköping University, 58183 Linköping, Sweden
[3]Materials Department, University of California Santa Barbara, Santa Barbara, California 93106, USA
[4]Leibniz Institut für Polymerforschung e.V., 01069 Dresden, Germany

[a)]Electronic mail: mhilfiker2@huskers.unl.edu; URL: http://ellipsometry.unl.edu

ABSTRACT

A set of monoclinic β-(Al$_x$Ga$_{1-x}$)$_2$O$_3$ films coherently grown by plasma-assisted molecular beam epitaxy onto (010)-oriented β-Ga$_2$O$_3$ substrates for compositions $x \leq 0.21$ is investigated by generalized spectroscopic ellipsometry at room temperature in the spectral range of 1.5 eV–9.0 eV. We present the composition dependence of the excitonic and band to band transition energy parameters using a previously described eigendielectric summation approach for β-Ga$_2$O$_3$ from the study by Mock *et al.* All energies shift to a shorter wavelength with the increasing Al content in accordance with the much larger fundamental band to band transition energies of Al$_2$O$_3$ regardless of crystal symmetry. The observed increase in the lowest band to band transition energy is in excellent agreement with recent theoretical predictions. The most important observation is that charge confinement in heterostructures will strongly depend on the growth condition due to the strongly anisotropic properties of the band to band transitions.

Published under license by AIP Publishing. https://doi.org/10.1063/1.5097780

Recent research interest has focused worldwide on β-Ga$_2$O$_3$ as the largest bandgap (4.8 eV–5.04 eV)[1–6] semiconductor that can also be melt grown in a single crystalline form.[7] Feasible *n*-type doping with tetravalent cations and a predicted breakdown electric field of more than double of the predicted limits for SiC and GaN envision tripling power performance of contemporary device structures in the very near future.[7] Heteroepitaxial growth of alloyed compounds with ultrawide bandgap Al$_2$O$_3$ (8.8 eV)[8] permits the creation of heterostructure devices, for example, exploiting valence and conduction band offsets for modulation-doped field effect transistors (MODFETs)[9–11] and two-dimensional electron gas formation.[12,13]

The phase diagram between the monoclinic crystal structure β-Ga$_2$O$_3$ and rhombohedral structure (trigonal; sapphire) α-Al$_2$O$_3$ predicts pure phase β–(Al$_x$Ga$_{1-x}$)$_2$O$_3$ for composition $x \leq 0.7$ for growth temperatures above the congruent point at $\approx$800 °C.[14] Fully coherent heterostructures with the composition up to $\approx$17% were demonstrated using plasma-assisted molecular beam epitaxy (PAMBE) on (010) oriented β-Ga$_2$O$_3$ substrates.[15]

Identification of the band to band transitions and excitonic contributions as a function of composition is highly desired for comparison with band structure calculations and for determination of, for example, band offsets and charge confinement. Recently, generalized spectroscopic ellipsometry was used to accurately determine the dielectric function tensor of the highly anisotropic monoclinic β-Ga$_2$O$_3$.[2,3,5] An eigendielectric summation approach was introduced by Sturm *et al.* to identify valence to conduction band electronic transitions, their strength and polarization directions (selection rules), and excitonic contributions, and comparison was given with density functional theory (DFT) results.[2,4,5]

For β-Ga$_2$O$_3$, the lowest energy band to band transition is polarized nearly parallel to lattice axis **c**, the second is polarized nearly parallel to **a**, and the third is polarized parallel to **b**.[2,5] Excitonic contributions and different band to band transition critical point (CP) parameters are the source of peculiar anisotropy in the near bandgap spectral region. Anisotropy, band to band transitions, selection rules, and excitonic properties have not been determined by experiment thus far for β–(Al$_x$Ga$_{1-x}$)$_2$O$_3$.

Feng *et al.* analyzed transmittance of β–(Al$_x$Ga$_{1-x}$)$_2$O$_3$ epitaxial films and reported bandgap values of 5.06 eV for $x = 12\%$ and 5.29 eV for $x = 35\%$ without polarization assignment.[16] Schmidt-Grund *et al.* determined an isotropically averaged dielectric function of β–(Al$_x$Ga$_{1-x}$)$_2$O$_3$ by spectroscopic ellipsometry from 0.5 eV to 8.5 eV for $x = 0.11$ to $x = 0.55$. A composition dependent, isotropically averaged bandgap energy was estimated using the onset of the absorption method.[17] Wang *et al.* reported on β–(Al$_x$Ga$_{1-x}$)$_2$O$_3$ obtained by cosputtering reaching Al compositions x up to 6%. Energy parameters estimated from the onset of absorption shift to higher photon energies with increasing x (4.89 eV–5.19 eV).[18] Krueger *et al.* investigated the bandgap energy parameters of powder samples produced by solution combustion synthesis using x-ray photo-electron spectroscopy (XPS) and DFT calculations. An approximately linear shift was reported between $x = 0$ and $x = 1$.[19] Polarization assignments and selection rules were not provided. Zhang *et al.* investigated XPS and the onset of absorption in pulsed laser deposition grown films covering the entire composition range. A strongly nonlinear shift was reported between $x = 0$ and $x = 1$.[20] A study of the onset of absorption combined with DFT calculations was performed for β–(Al$_x$Ga$_{1-x}$)$_2$O$_3$ films grown by laser molecular beam epitaxy (LMBE) on ($\bar{2}$01) β-Ga$_2$O$_3$ substrates for $x \leq 0.54$.[21] Absorption edge estimated bandgap energy parameters were also reported to shift linearly for corundum α–(Al$_x$Ga$_{1-x}$)$_2$O$_3$ deposited by spray assisted mist chemical vapor deposition.[25,26]

Fares *et al.* determined the valence and conduction band offsets between Al$_2$O$_3$ grown by atomic layer deposition and MBE deposited β–(Al$_{0.14}$Ga$_{0.86}$)$_2$O$_3$ using XPS. A type-I alignment was reported for the valence band offset (0.23 eV) and good electron confinement conditions for the conduction band offset (1.67 eV). Polarization dependencies of band offsets were not discussed.[22] Peelaers *et al.*[23] and Wang *et al.*[24] performed a detailed DFT study of fully relaxed (unstrained) (Al$_x$Ga$_{1-x}$)$_2$O$_3$ alloys in both monoclinic and hexagonal phases using a hybrid DFT functional. Composition dependencies of formation enthalpies, band alignment with respect to the vacuum level, and bandgap energies were studied, with the latter defined as the difference between band edges at the Γ point (direct) and the valence band maximum close to the L point in the Brillouin zone and the conduction band minimum at the Γ point (indirect). Both groups reported qualitatively consistent results with a slightly nonlinear parabolic (bowing) dependence of the bandgap energy vs composition.

It is of interest to note that all thus far available band to band transition energy parameters were determined from either optical techniques (onset of absorption) or XPS lineshape analyses without consideration of the anisotropic properties of the electronic transitions in the near bandgap spectral region. Furthermore, it appears that exciton formation which reduces the energy of the onset of absorption was not yet accounted for in data analysis of optical spectra of β–(Al$_x$Ga$_{1-x}$)$_2$O$_3$. In this paper, we report the investigation of a set of heteroepitaxial films of pure phase monoclinic β–(Al$_x$Ga$_{1-x}$)$_2$O$_3$ coherently grown by plasma-assisted MBE (PAMBE) onto (010) oriented β-Ga$_2$O$_3$ substrates for compositions $x \leq 0.21$ by generalized spectroscopic ellipsometry at room temperature in the spectral range of 1.5 eV–9.0 eV. We employ our recently developed eigendielectric summation approach, and we report anisotropy, band to band transitions, selection rules, and excitonic properties for compositions $x \leq 0.21$.

Nominally undoped β–(Al$_x$Ga$_{1-x}$)$_2$O$_3$ films were grown on (010) β-Ga$_2$O$_3$ substrates at 600 °C–700 °C by PAMBE. Composition determination of the coherently grown epitaxial films was performed by X-ray diffraction (XRD) as discussed by Oshima *et al.*[15] The β–(Al$_x$Ga$_{1-x}$)$_2$O$_3$ films were grown under slight metal rich conditions with a similar Ga flux of 1×10^{-7} Torr while the Al flux was varied from 0.9×10^{-8} to 1.1×10^{-8} Torr for different Al compositions in the films. Further details of the XRD investigations are given in the supplementary material.

We measured room temperature generalized spectroscopic ellipsometry data in the Mueller matrix[27] presentation in the spectral range from 1.5 eV to 9.0 eV. A rotating-analyzer ellipsometer with an automated compensator function (VUV-VASE, J. A. Woollam Co., Inc.) was used for the vacuum-ultraviolet (VUV) spectral region. Data were acquired at three angles of incidence ($\Phi_a = 50°$, 60°, and 70°) and at several azimuth angles by manually rotating the sample about the sample normal in steps of $\approx 45°$. A dual-rotating compensator ellipsometer (RC2, J. A. Woollam Co., Inc.) with the automated sample rotation function was used to obtain data in the remaining spectral region. Measurements were taken at three angles of incidence ($\Phi_a = 50°$, 60°, and 70°) and at one full sample rotation in steps of 15°. Note that data acquisition with the RC2 instrument is much faster due to the multiple-wavelength [charge-coupled device (CCD) light detection] operation design while also providing access to the full Mueller matrix elements. The VUV instrument is a rotating turret-based single-detector, single-wavelength design, and does not permit acquisition of the 4th row of the Mueller matrix. Because the β–(Al$_x$Ga$_{1-x}$)$_2$O$_3$ films are neither magnetically nor optically active, the Mueller matrix is symmetric in all elements, and loss of information about the 4th row in the VUV spectral range does not impair access to the dielectric function tensor.

Ellipsometry is an indirect technique, and best match model calculations are needed. Here, we employ the substrate-film(layer)-roughness(layer)-ambient model.[27] For the β-Ga$_2$O$_3$ substrate and β–(Al$_x$Ga$_{1-x}$)$_2$O$_3$ film, we choose a coordinate system common to both, as described in Ref. 5. Then, x is parallel to lattice axis **a**, y is parallel to **c***, where the plane defined by **a** and **c*** is the monoclinic plane, and z is parallel to **b** yielding the dielectric tensor[28]

$$\varepsilon = \begin{pmatrix} \varepsilon_{xx} & \varepsilon_{xy} & 0 \\ \varepsilon_{xy} & \varepsilon_{yy} & 0 \\ 0 & 0 & \varepsilon_{zz} \end{pmatrix}. \tag{1}$$

We previously reported detailed determination of this tensor for β-Ga$_2$O$_3$, and we provided an eigendielectric vector summation approach to analyze the spectral behavior of this tensor to identify and determine band to band transition and excitonic properties.[5] We use the same approach and the same functions to describe the tensor for β–(Al$_x$Ga$_{1-x}$)$_2$O$_3$. Here, the optical effect of the substrate is calculated using the parameter set given in Ref. 5. The tensor for β–(Al$_x$Ga$_{1-x}$)$_2$O$_3$ has the same shape as in Eq. (1). Due to the coherent growth, the axes **a**, **c***, and **b** are parallel within the substrate and the epitaxial film. The effect of roughness is accounted for by a thin model layer with an isotropic average over all β–(Al$_x$Ga$_{1-x}$)$_2$O$_3$ tensor elements and weighted with 50% void, as described in Ref. 5. A wavelength by wavelength approach as utilized previously to simultaneously best-model match calculated data to sets of data obtained from samples with the same physical properties but different surface orientations is not possible

here. Hence, to determine the dielectric tensor elements for the epitaxial films, ε_{xx}, ε_{yy}, ε_{xy}, and ε_{zz}, we use the CP model dielectric functions (MDF) projected into tensor dyadics as described by Mock *et al.* for the best match model calculations. However, to account for the changes in the band structure of β-Ga$_2$O$_3$ upon introduction of Al, we initially permit all parameters to vary. From the parameters of these oscillator functions, amplitude, broadening, excitonic energy, transition energies, and their eigendielectric polarization orientation are determined. The best match ellipsometry model parameters for the β–(Al$_x$Ga$_{1-x}$)$_2$O$_3$ film thickness and roughness layer thickness are 82.(3) nm and 1.(2) nm for the 12% sample, 120.(7) nm and 1.(9) nm for the 15% sample, and 63.(0) nm and 1.(2) nm for the 21% sample, respectively. The last digit which is determined within the 90% confidence interval is indicated with parentheses.

Selected experimental and best match model calculated Mueller matrix data are shown in the supplementary material. An excellent match between all experimental and model data for all investigated samples is obtained. Figure 1 depicts the best match model calculated MDF tensor element spectra for β–(Al$_{0.12}$Ga$_{0.88}$)$_2$O$_3$, as an example (solid lines). Included for comparison are data obtained for β-Ga$_2$O$_3$ previously (dashed lines).[2,5] Table I summarizes all CP MDF parameters for the contributions polarized within the monoclinic plane for the sample with $x = 12\%$, as an example. Further data are listed in the supplementary material. We note that limited sensitivity was observed for the CP MDF parameters in ε_{zz} for photon energies above approximately 7 eV (MDF parameters for CP$_2^b$ and CP$_3^b$). Hence, we have kept these parameters constant. We also note that we observed limited sensitivity to the energy levels of the excitonic contributions. Hence, we kept the differences between energy parameters of CP$_{0x}^{ac}$ − CP$_0^{ac}$ = 120 meV, CP$_{1x}^{ac}$ − CP$_1^{ac}$ = 230 meV, and CP$_{0x}^b$ − CP$_0^b$ = 178 meV, i.e., the exciton binding energy parameters, constant at those observed for β-Ga$_2$O$_3$ for all x investigated here. Finally, due to the blue shift of all CP contributions, we note that CP$_6^{ac}$ moved outside the spectral range and was omitted due to the lack of sensitivity to its parameters,
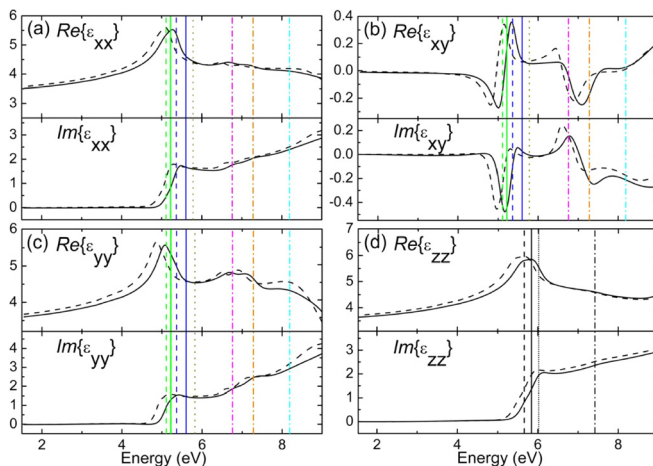
TABLE I. Example for CP MDF tensor parameters for the eigendielectric summation approach for contributions in the **a-c** plane determined in this work for β-(Al$_{0.12}$Ga$_{0.88}$)$_2$O$_3$. See Ref. 5 for the parameter definition. X-ray diffraction reciprocal space mapping data included within the supplementary material suggest that all films investigated here are coherently strained without relaxation. The last digit which is determined within the 90% confidence interval is indicated with parentheses.

	α (°)	A (eV)	E (eV)	B (eV)	b (eV)
CP$_{0x}^{ac}$	120.5 (4)	1.26 (6)	5.10 (7)	0.42 (4)	0.50 (4)
CP$_0^{ac}$	120.5 (4)	19.4 (4)	5.22 (0)	0.02 (9)	…
CP$_{1x}^{ac}$	25.8 (7)	1.50 (1)	5.36 (1)	0.43 (4)	0.48 (8)
CP$_1^{ac}$	25.8 (7)	26.9 (3)	5.59 (8)	0.09 (4)	…
CP$_2^{ac}$	166.1 (2)	0.20 (6)	5.78 (9)	0.93 (6)	…
CP$_3^{ac}$	51.8 (7)	1.06 (8)	6.75 (8)	0.48 (9)	0.09 (3)
CP$_4^{ac}$	118.9 (5)	1.97 (8)	7.28 (3)	0.73 (0)	0.22 (1)
CP$_5^{ac}$	111.2 (6)	2.70 (1)	8.19 (0)	2.20 (2)	2.65 (0)
CP$_7^{ac}$	109.9 (7)	2.59 (7)	11.17 (1)	8.74 (4)	…
CP$_8^{ac}$	22.9 (9)	3.58 (2)	12.34 (3)	7.61 (0)	…

and its contributions are compensated by its next nearest CP structure, CP$_5^{ac}$.

In Fig. 1, most features appear shifted toward higher energies upon the incorporation of Al. The identified energies of the CP contributions are indicated by vertical lines. Color and line styles are identical to those shown in Fig. 2, where all CP energies are summarized for all samples investigated. In Figs. 1(a) (ε_{xx}), 1(c) (ε_{yy}), and 1(d) (ε_{zz}), it can be seen that the blue shift of the onset of absorption and the maximum in the real part of the dielectric functions along the crystal directions **a**, **c***, and **b**, respectively, also results in a reduction of the real parts within the bandgap spectral region. This reduction is consistent with the observation made by Schmidt-Grund *et al.* albeit their MDF
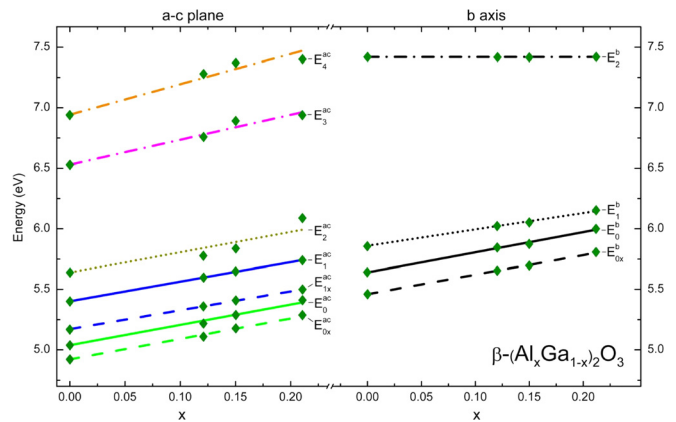

FIG. 1. Real and imaginary components of the dielectric tensor elements, ε_{xx}, ε_{yy}, ε_{xy}, and ε_{zz} for β-(Al$_{0.12}$Ga$_{0.88}$)$_2$O$_3$ (solid lines) in comparison with β-Ga$_2$O$_3$ (dashed lines). Vertical lines indicate transition energies for the sample with a 12% Al content, consistent with the color and style shown in Fig. 2.

FIG. 2. Transition energies (symbols) vs Al content x of β-(Al$_x$Ga$_{1-x}$)$_2$O$_3$ films determined by CP MDF analysis (for respective CP MDF definitions, labeled here by lines with different styles as indicated, and contributions for β-Ga$_2$O$_3$ also shown here, see Ref. 5.): dashed-lines: exciton transitions; solid lines: near bandgap band to band transitions; dotted lines: above bandgap transitions; dash-dotted lines: higher energy transitions. The uncertainty limits determined within the 90% confidence interval, which are smaller than the symbol sizes, are given in Table I and in the supplementary material.

was an isotropic average over all crystal directions. The systematic blue shift of all band to band transitions is summarized in Fig. 2, where the left side shows the CP transitions within the monoclinic plane, and the right panel lists those for polarization parallel to axis **b**. Lines are linear approximations to the composition dependence of the CP energy parameters observed in this work. The solid lines indicate the lowest three band to band transitions (E_0^{ac}, E_1^{ac}, E_0^b), which shift nearly parallel for $x \leq 0.21$. Figure 3 depicts the shift in the lowest bandgap parameter observed here (E_0^{ac}) in comparison with the lowest band to band transition energy parameters reported from DFT calculations by Wang et al.[24] and Peelaers et al.[23] While slight bowing was predicted in the previous DFT work, the dashed line is a reasonable linear approximation to our data for the composition range investigated here.

We note excellent agreement between theory and experiment, where the remaining differences may be caused by the influence of strain within our epitaxial films, and which was not considered by the calculations reported by Wang et al. and Peelaers et al. We note at this point that the strain will also depend on the surface orientation at which a given film is grown. Our films are grown fully coherently onto the (010) substrates. Reciprocal x-ray reflection space mapping data in the supplementary material also rule out any lattice relaxation. Hence, the state of strain is fully defined in all of our films. DFT provided reliable stiffness tensor elements to calculate stress.[4] However, the linear deformation potential parameters as well as the linear pressure potential parameters for band to band transitions in β–$(Al_xGa_{1-x})_2O_3$ have not been determined yet. Therefore, presently, we cannot further disentangle the effect of alloying with strain or stress yet. Investigations of fully strained films on different substrate surfaces will be needed in the future.

In summary, we have determined the anisotropic dielectric function tensor elements of a set of β–$(Al_xGa_{1-x})_2O_3$ films grown coherently at the (010) surface of β-Ga_2O_3 substrates by plasma-assisted MBE using generalized spectroscopic ellipsometry in the spectral range from 1.5 eV to 9.0 eV. We have analyzed the ellipsometry data using our previously developed critical point model dielectric function
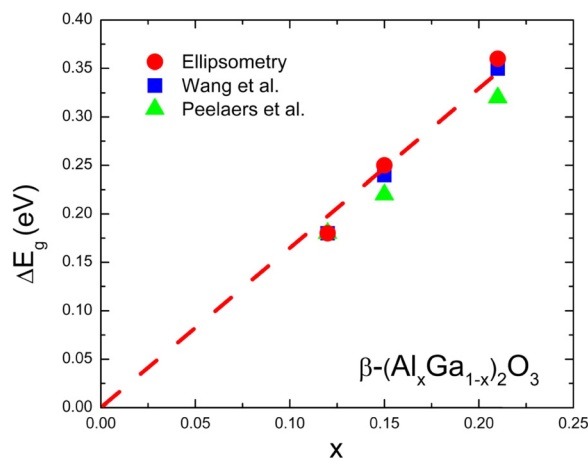
approach for monoclinic symmetry semiconductor materials, and we have reported the composition dependence of the lowest energy band to band transitions and their polarization directions. Our results are relevant for the evaluation of band offsets and design of electron confinement in β–$(Al_xGa_{1-x})_2O_3$–β-Ga_2O_3 heterostructures, where the direction dependence of the band structure must be considered accordingly. The observed increase in the lowest band to band transition energy is in excellent agreement with recent theoretical predictions, which suggests that strain in coherent growth may play a minor role for films with Al contents investigated here.

See the supplementary material for the details of the samples investigated, the experimental procedures, and the numerical values of all parameters determined in this work.

REFERENCES

[1]C. Janowitz, V. Scherer, M. Mohamed, A. Krapf, H. Dwelk, R. Manzke, Z. Galazka, R. Uecker, K. Irmscher, R. Fornari, M. Michling, D. Schmeißer, J. R. Weber, J. B. Varley, and C. G. V. de Walle, New J. Phys. **13**, 085014 (2011).

[2]C. Sturm, R. Schmidt-Grund, C. Kranert, J. Furthmüller, F. Bechstedt, and M. Grundmann, Phys. Rev. B **94**, 035148 (2016).

[3]C. Sturm, J. Furthmüller, F. Bechstedt, R. Schmidt-Grund, and M. Grundmann, APL Mater. **3**, 106106 (2015).

[4]J. Furthmüller and F. Bechstedt, Phys. Rev. B **93**, 115204 (2016).

[5]A. Mock, R. Korlacki, C. Briley, V. Darakchieva, B. Monemar, Y. Kumagai, K. Goto, M. Higashiwaki, and M. Schubert, Phys. Rev. B **96**, 245205 (2017).

[6]Z. Galazka, Semicond. Sci. Technol. **33**, 113001 (2018).

[7]M. Higashiwaki and G. H. Jessen, Appl. Phys. Lett. **112**, 060401 (2018).

[8]R. H. French, J. Am. Ceram. Soc. **73**, 477 (1990).

[9]E. Ahmadi, O. S. Koksaldi, X. Zheng, T. Mates, Y. Oshima, U. Mishra, and J. S. Speck, Appl. Phys. Express **10**, 071101 (2017).

[10]Y. Zhang, C. Joishi, Z. Xia, M. Brenner, S. Lodha, and S. Rajan, Appl. Phys. Lett. **112**, 233503 (2018).

[11]S. Krishnamoorthy, Z. Xia, C. Joishi, Y. Zhang, J. McGlone, J. Johnson, M. Brenner, A. R. Arehart, J. Hwang, S. Lodha, and S. Rajan, Appl. Phys. Lett. **111**, 023502 (2017).

[12]T. Oshima, Y. Kato, N. Kawano, A. Kuramata, S. Yamakoshi, S. Fujita, T. Oishi, and M. Kasu, Appl. Phys. Express **10**, 035701 (2017).

[13]Y. Zhang, A. Neal, Z. Xia, C. Joishi, J. M. Johnson, Y. Zheng, S. Bajaj, M. Brenner, D. Dorsey, K. Chabak, G. Jessen, J. Hwang, S. Mou, J. P. Heremans, and S. Rajan, Appl. Phys. Lett. **112**, 173502 (2018).

[14]V. G. Hill, R. Roy, and E. F. Osborn, J. Am. Ceram. Soc. **35**, 135 (1952).

[15]Y. Oshima, E. Ahmadi, S. C. Badescu, F. Wu, and J. Speck, Appl. Phys. Express **31**, 061102 (2016).

FIG. 3. Shift of the lowest band to band transition in β-$(Al_xGa_{1-x})_2O_3$ relative to β-Ga_2O_3, $E_0^{ab}(x>0)-E_0^{ab}(x=0)$ (this work), and calculation results by Wang et al.[24] and Peelaers et al.[23] The dashed line is a linear approximation.

[16]Q. Feng, X. Li, G. Han, L. Huang, W. T. F. Li, J. Zhang, and Y. Hao, Opt. Mater. Express **7**, 1240 (2017).

[17]R. Schmidt-Grund, C. Kranert, H. von Wenckstern, V. Zviagin, M. Lorenz, and M. Grundmann, J. Appl. Phys. **117**, 165307 (2015).

[18]C. Wang, S. Yuan, S. Ou, S. Huang, K. Lin, Y. Chen, P. Hsiao, and D. Wuu, J. Alloys Compd. **765**, 894 (2018).

[19]B. Krueger, C. Dandeneau, E. Nelson, S. Dunham, F. Ohuchi, and M. Olmstead, J. Am. Ceram. Soc. **99**, 2467 (2016).

[20]F. Zhang, K. Saito, T. Tanaka, M. Nishio, M. Arita, and Q. Guo, Appl. Phys. Lett. **105**, 162107 (2014).

[21]J. Li, X. Chen, T. Ma, X. Cui, F.-F. Ren, S. Gu, R. Zhang, Y. Zheng, S. P. Ringer, L. Fu, H. H. Tan, C. Jagadish, and J. Ye, Appl. Phys. Lett. **113**, 041901 (2018).

[22]C. Fares, F. Ren, E. Lambers, D. C. Hays, B. P. Gila, and S. J. Pearton, J. Electron. Mater. **48**, 1568 (2019).

[23]H. Peelaers, J. B. Varley, J. S. Speck, and C. G. Van de Walle, Appl. Phys. Lett. **112**, 242101 (2018).

[24]T. Wang, W. Li, C. Ni, and A. Janotti, Phys. Rev. Appl. **10**, 011003 (2018).

[25]H. Ito, K. Kaneko, and S. Fujita, Jpn. J. Appl. Phys. Part 1 **51**, 100207 (2012).

[26]G. T. Dang, T. Yasuoka, Y. Tagashira, T. Tadokoro, W. Theiss, and T. Kawaharamura, Appl. Phys. Lett. **113**, 062102 (2018).

[27]H. Fujiwara, *Spectroscopic Ellipsometry* (John Wiley & Sons, New York, 2007).

[28]In this coordinate choice, $\mathbf{c}\star$ is defined perpendicular to the $\mathbf{a}$–$\mathbf{b}$ plane for convenience, while $\mathbf{c}$ shares the monoclinic angle $\beta = 103.7°$ with $\mathbf{a}$. See also Ref. 5.